Femtosecond Two-Dimensional Spectroscopy of Molecular Motion in Liquids

Thomas Steffen and Koos Duppen
Ultrafast Laser and Spectroscopy Laboratory, Department of Chemistry, Materials Science Center,
University of Groningen, Nijenborgh 4, 9749 AG Groningen, the Netherlands

(Received 20 September 1995)

Intermolecular motion in CS_2 and benzene is investigated by femtosecond nonresonant four- and six-wave mixing. Impulsive stimulated six-wave mixing yields new information on dephasing of coherent nuclear motion, not accessible from four-wave mixing experiments. The results cannot be modeled by two independent harmonic modes accounting for coherent librations and rotational diffusion.

PACS numbers: 33.70.Jg, 33.15.Vb, 42.50.Md, 78.47.+p

Ultrashort laser pulses, with durations of less than 100 fs, are very capable of exciting nuclear motion in liquids on time scales that are short compared to typical collisional periods [1–4]. This opens the possibility to investigate the static and dynamical properties of local structures in liquids by coherent spectroscopic techniques in real time. The memory function of the system that is generally unknown and presumably quite complex for liquids can be determined when a sequence of pulses is applied. We report here on fifth-order nonlinear optical experiments that are designed to directly probe the relevant memory times of nuclear propagation, by trying to rephase macroscopic nuclear coherence after a well-defined period of dephasing.

Molecular motion in transparent liquids has been investigated intensively by frequency-domain experiments such as dynamic light scattering [5] and by time-domain experiments such as the optical Kerr effect (OKE) [1,2] and transient grating scattering (TGS) [3,4]. The information, obtained by these techniques, is in principle equivalent [6]. Since the OKE and TGS signals depend on a single time variable, the short- and long-lived components of the total memory function cannot be separated [7]. To determine the character of the underlying microscopic processes in the liquid, higher-order nonlinear optical experiments are required that allow for independent change of several propagation times.

The Raman-echo, recently performed by Vanden Bout, Muller, and Berg [8] and by Inaba *et al.* [9], was the first example of such a higher-order nonlinear experiment in liquids. Since in these picosecond experiments a single intramolecular vibrational state is excited, this seventh-order nonlinear Raman effect can be directly compared to a resonant photon echo experiment on a two-level system [10,11]. Rephasing of vibrational coherence into an echo occurs when there are slow fluctuations (e.g., inhomogeneous broadening) in the propagation of the system.

Impulsive excitation with femtosecond pulses gives rise to an entirely different situation. The ultrafast pulses cover a broad range of low-frequency transitions, and the molecules can no longer be described as two-level systems. This situation has been described first by Tanimura and Mukamel [12], who calculated the higher-order nonlinear optical response of a nuclear harmonic mode using path-integral techniques in Liouville space.

Recently, the first impulsive fifth-order nonlinear experiments were reported by Tominaga *et al.* [13,14]. According to their observations, the fifth-order response of CS_2 resembles, along both time variables, the nuclear part of the third-order TGS response: It consists of an inertial coherent contribution that rises and falls in the subpicosecond range, followed by a slow diffusive tail. In their analysis, based on the theory of Ref. [12], they assumed that the molecular dynamics is dominated by two independent contributions: a homogeneously broadened underdamped mode to model coherent librations and an overdamped mode accounting for diffusive reorientation. Both the third- and fifth-order results were reported to be well described by the theory.

We present here results of fifth-order experiments on CS_2 and benzene. Both samples show qualitatively the same features. In contrast to Ref. [13], the shape of the fifth-order signals is found to be different from that of third-order TGS signals when either of the two delay times is changed. We further demonstrate that current theoretical models fail to explain the full two-dimensional fifth-order response correctly. In agreement with Tominaga and Yoshihara [13] we find indications for homogeneous broadening of ultrafast librational motion. However, this conclusion should be considered with caution, since the employed model fails to explain all observations.

The principle of the experiment, depicted schematically in Fig. 1, is the same as that of Ref. [13], but with a slightly modified beam configuration. Two pairs of coincident femtosecond pulses with wave vector $\boldsymbol{k}_1$ and $\boldsymbol{k}_2$ and a mutual delay t_1 excite the sample. After a variable delay t_2 with respect to the second pulse pair, a fifth pulse with wave vector $\boldsymbol{k}_{\mathrm{pr}}$ converts the propagating intermolecular coherent state into an optical signal with wave vector $\boldsymbol{k}_5 = \boldsymbol{k}_{\mathrm{pr}} + 2(\boldsymbol{k}_1 - \boldsymbol{k}_2)$. The pulses, with a central wavelength of 620 nm and a duration of 45 fs, were generated with an amplified CPM-laser system operating at 9 kHz [11]. They were focused in a 1 mm path length, room temperature sample with a

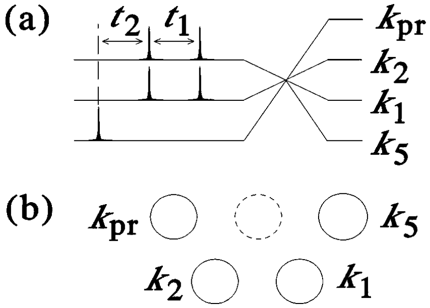

FIG. 1. (a) Layout of the time-domain fifth-order experiment. Two subsequent pulse pairs, separated by delay time t_1, impulsively excite molecular motion. After a delay t_2 a probe pulse generates an optical signal with wave vector $\mathbf{k}_5 = \mathbf{k}_{pr} + 2(\mathbf{k}_1 - \mathbf{k}_2)$. (b) Spatial configuration of the beams. The dashed circle gives the position of the third-order grating scattering (TGS) signal wave vector $\mathbf{k}_{TGS} = \mathbf{k}_{pr} + (\mathbf{k}_1 - \mathbf{k}_2)$.

150 mm focal length lens. The angle between adjacent beams was about 45 mrad. The total applied energy per five-pulse cycle was kept smaller than 300 nJ for CS_2 and 600 nJ for benzene, in order to avoid self-focusing and continuum generation. The pulses with wave vector $\mathbf{k}_2$ were polarized horizontally, the pulses $\mathbf{k}_1$ and $\mathbf{k}_{pr}$ were polarized vertically. The signal was spatially filtered, transmitted through a vertically oriented polarizer, detected by a photomultiplier, and processed by a lock-in amplifier. It depends on all five pulses, is vertically polarized (in our configuration third- and fifth-order polarizations are orthogonal), and has a 4.9 ± 0.3 power dependence. The shape of the signal does not depend on the intensity.

In Fig. 2(a) the fifth-order response of CS_2 is shown for variable delay t_2 and fixed t_1 together with the third-order grating signal that was measured in the direction $\mathbf{k}_{TGS} = \mathbf{k}_{pr} + (\mathbf{k}_1 - \mathbf{k}_2)$ when the first pulse pair was blocked. It is clear that third- and fifth-order responses differ considerably: The coherent artifact in the TGS signal around zero delay that results from nonresonant excitation of electrons to virtual states (electronic hyperpolarizability) is absent in the fifth-order traces. Such artifacts were observed by Tominaga and Yoshihara [13] in their fifth-order experiments, around $t_2 = -t_1$ and weakly around $t_2 = 0$. From the intensity dependence it followed that these were due to lower-order grating scattering contributions [14]. In our case such signals are absent due to the different beam configuration, and hence the pure fifth-order response is measured. We further find that there is no exponential tail due to diffusive reorientation in the t_2 dependence of the fifth-order experiment. As shown in Fig. 2(b) for benzene, the position and shape of the signals do not depend on the delay time t_1.

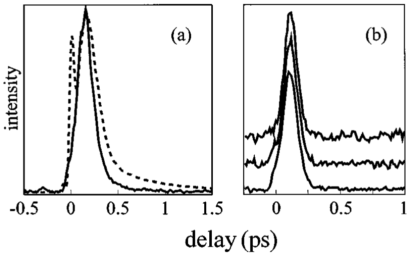

FIG. 2. (a) Fifth-order signal of CS_2 as a function of delay time t_2 for $t_1 = 300$ fs. Comparison with the third-order TGS signal (dashed line) shows that diffusion is absent in the fifth-order trace. (b) The shape and position of the fifth-order signal for variable delay t_2 is independent of t_1, as shown for benzene for $t_1 = 0.5, 1.0, 1.5$ ps (from bottom to top).

The fifth-order signals for variable delay t_1 and fixed t_2 are presented in Fig. 3(a). The traces show fast nonexponential behavior followed by single exponential decay with a decay constant of 1.6 ± 0.1 ps for CS_2 and 2.5 ± 0.2 ps for benzene. These features are typical for the optically heterodyned detected optical Kerr effect and for the square root of the TGS signal, instead of for the TGS signal itself. The t_1 dependence of CS_2 was only briefly discussed in Refs. [13] and [14], but no experimental results were shown. The difference between the t_2 dependence of the fifth-order response and the third-order TGS signal was not noticed in those papers, possibly because of the lower time resolution that causes spectral filter effects [1].

Formal expressions for the third-order nonlinear optical response under electronically nonresonant excitation have been derived by Hellwarth by evoking the Born-Oppenheimer approximation [6]. The coupling between the light field and the modes q of the system is then governed by the electronic polarizability $\chi(q)$. These calculations are easily extended to describe fifth-order nonlinear processes [12,15]. The third- and fifth-order polarization $P^{(3)}(t)$ and $P^{(5)}(t)$ can be written in terms of the corresponding response functions $R^{(3)}(\tau_1)$ and $R^{(5)}(\tau_2, \tau_1)$ [6,15,16],

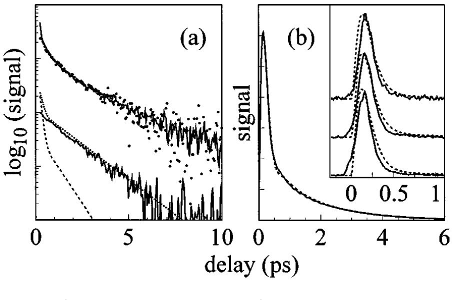

FIG. 3. (a) Fifth-order signals of benzene (upper solid line) and CS_2 (lower solid line) as a function of delay time t_1 for $t_2 = 150$ fs. The signals resemble the third-order heterodyned OKE effect (shown for benzene as the dotted trace), but are not described by the simulations (shown for CS_2 as the long dashed line). The *amplitude* of the calculated signal (short dashed line) agrees with the *intensity* of the measured signal. This is not explained by the model. (b) The deconvoluted third-order heterodyned OKE signal of CS_2 (solid line) and its simulation (dashed line). In the inset, the measured t_2 dependence of the fifth-order signal of CS_2 (solid lines, $t_1 = 0.3, 0.6, 0.9$ ps from bottom to top) is shown together with the calculated responses (dashed lines).

$$P^{(3)}(t) = E(t - t_1)\int_0^\infty d\tau_1\, R^{(3)}(\tau_1)E^2(t - \tau_1)\,, \qquad (1)$$

$$\begin{aligned} P^{(5)}(t) = {} & E(t - t_2 - t_1)\int_0^\infty d\tau_2 \\ & \times \int_0^\infty d\tau_1\, R^{(5)}(\tau_2, \tau_1) \\ & \times E^2(t - t_1 - \tau_2)E^2(t - \tau_2 - \tau_1)\,. \end{aligned} \qquad (2)$$

Here, we suppressed an explicit tensor treatment of the material response. The integration along the propagation times τ_1 and τ_2 between subsequent interactions accounts for the effects of finite pulse width. The observed signals are proportional to the absolute square of the polarizations integrated over time t. The response functions $R^{(3)}$ and $R^{(5)}$ can be expressed by commutators of the electronic polarizability operator in the interaction picture, $\tilde{\chi}(q)$ [6,15,16],

$$\begin{aligned} R^{(3)}(\tau_1) = {} & \frac{-i}{2\hbar}\langle[\tilde{\chi}(\tau_1), \tilde{\chi}(0)]\rangle \\ = {} & \frac{1}{\hbar}\sum_{k,l} P(k)\langle k|\chi(q)|l\rangle\langle l|\chi(q)|k\rangle e^{-\Gamma_{kl}\tau_1} \\ & \times \sin\omega_{kl}\tau_1\,, \end{aligned} \qquad (3)$$

$$\begin{aligned} R^{(5)}(\tau_2, \tau_1) = {} & \frac{-1}{4\hbar^2}\langle[[\tilde{\chi}(\tau_2 + \tau_1), \tilde{\chi}(\tau_1)], \tilde{\chi}(0)]\rangle = \frac{-1}{2\hbar^2}\sum_{k,l,m} P(k)\langle k|\chi(q)|l\rangle\langle l|\chi(q)|m\rangle\langle m|\chi(q)|k\rangle e^{-\Gamma_{kl}\tau_1} \\ & \times \{e^{-\Gamma_{km}\tau_2}\cos(\omega_{kl}\tau_1 + \omega_{km}\tau_2) - e^{-\Gamma_{ml}\tau_2}\cos(\omega_{kl}\tau_1 + \omega_{ml}\tau_2)\}\,. \end{aligned} \qquad (4)$$

Here, $|k\rangle$, $|l\rangle$, and $|m\rangle$ are energy eigenstates of the system, $P(k)$ denotes a thermal distribution over initial states $|k\rangle$, and damping is introduced in the weak coupling limit by writing the difference of the energy eigenvalues as $\varepsilon_i - \varepsilon_j \equiv \omega_{ij} + i\Gamma_{ij} = \omega_{ij} + i[\Gamma_{ij}^* + \frac{1}{2}\gamma_i + \frac{1}{2}\gamma_j]$. Γ_{ij}^* and γ_i describe dephasing of the coherence $|i\rangle\langle j|$ and decay of the population $|i\rangle\langle i|$, respectively. Note that the treatment at this stage is independent of the Hamiltonian of the system and of the form of the polarizability operator.

For a harmonic Hamiltonian, the eigenstates are known and the coordinate q can be expressed in terms of raising and lowering operators $a^\dagger$ and a. When the polarizability operator χ depends linearly on q, the highest-order optical nonlinearity is the third-order response [12]. Hence, to describe fifth-order experiments in harmonic systems, we have to expand $\chi(q)$ up to second order in q: $\chi(q) = c_1 q + c_2 q^2$. Since the action of a and $a^\dagger$ on the eigenstates is known, Eqs. (3) and (4) are easily evaluated,

$$R^{(3)}(\tau_1) = \frac{c_1^2}{2m\omega}e^{-\Gamma_1\tau_1}\sin\omega\tau_1 + \left(\frac{c_2}{2m\omega}\right)^2 2\hbar f(T)e^{-\Gamma_2\tau_1}\sin 2\omega\tau_1\,, \qquad (5)$$

$$\begin{aligned} R^{(5)}(\tau_2, \tau_1) = {} & \left(\frac{c_2}{m\omega}\right)^3 2\hbar f(T)e^{-\Gamma_2\tau_1}[e^{-\Gamma_2\tau_2}\cos 2\omega(\tau_2 + \tau_1) - e^{-\gamma\tau_2}\cos 2\omega\tau_1] \\ & + c_2\left(\frac{c_1}{m\omega}\right)^2 e^{-\Gamma_1\tau_1}\{e^{-\Gamma_2\tau_2}\cos\omega(\tau_1 + 2\tau_2) - e^{-\gamma\tau_2}\cos\omega\tau_1 \\ & + e^{-\Gamma_1\tau_2}[\cos\omega(\tau_1 + \tau_2) - \cos\omega(\tau_1 - \tau_2)]\}\,. \end{aligned} \qquad (6)$$

Here, Γ_1, Γ_2, and γ are the state independent dephasing rates of one- and two-quantum coherences and the population decay, respectively. $f(T)$ is a temperature dependent factor that depends on the initial distribution of occupied states $P(k)$. In the limit of frequency-independent damping and provided $\Gamma_1 = \frac{1}{2}\Gamma_2 = \frac{1}{2}\gamma$ holds, the second part of Eq. (6) agrees with the work of Tanimura and Mukamel [12], who avoided the assumption of weak coupling by explicitly including Brownian oscillators, but it differs from expressions given by Leegwater and Mukamel [17]. A detailed comparison between the various models will be published elsewhere [15].

The fifth-order response function is sensitive to the memory times of the propagation [12]. In the static (inhomogeneous) limit, the nonlinear polarizations Eqs. (1) and (2) have to be integrated over a distribution of transition frequencies ω. For large inhomogeneous width, all terms of $R^{(5)}$ are negligible compared to the last one that reaches its maximum at $\tau_2 = \tau_1$. This term arises from the excitation of a one-quantum coherence $|k\rangle\langle k + l|$ by the first pulse pair, which through a two-quantum transition is converted into the coherence $|k + 2\rangle\langle k + l|$ by the second pulse pair. The system then acquires phases $\exp(i\omega\tau_1)$ and $\exp(-i\omega\tau_2)$ during the first and second propagation periods, respectively. When τ_2 equals τ_1, the phases of the two propagation periods compensate for each other, independent of the frequency. The nuclear coherence is then recovered, the signal reaches its maximum value, and hence it can be called a motional echo. For homogeneous dephasing, the fifth-order signal reaches its maximum directly after the second pulse pair.

Echo-type behavior was not observed for CS_2 and benzene. Instead, as depicted in Figs. 2(b) and 3(b), the signal for variable t_2 always rises directly after the second pulse pair, irrespective of delay time t_1. This indicates that inhomogeneous broadening is insignificant for intermolecular motion in these systems. We follow Tominaga and Yoshihara [13] and use two independent harmonic modes, one overdamped and one underdamped, to stimulate the signals. In case the damping rate is comparable to or larger than the frequency of the mode, the weak-coupling limit for the damping does not hold. Coupling with Brownian oscillators can then be used to overcome this problem [12]. For an underdamped mode ($\omega > \Gamma_1, 2\omega > \Gamma_2$), ω and 2ω in Eqs. (5) and (6) should be replaced by $\Omega = (\omega_2^2 - \Gamma_1^2/4)^{1/2}$ and $2\Omega = (4\omega^2 - \Gamma_2^2/4)^{1/2}$, respectively. For an overdamped mode ($\omega < \Gamma_1,\ 2\omega < \Gamma_2$), the response functions are to be continued analytically. Because the two modes are assumed to be independent, the total response function is simply the sum of both contributions of the form of Eqs. (5) and (6).

We fitted the third-order nuclear response of CS_2, obtained from OKE measurements using unamplified CPM-laser pulses and a setup as described in Ref. [1]. Based on the parameters of this fit, we calculated the t_1 and t_2 dependence of the fifth-order experiments. The relative amplitudes for the homogeneously broadened underdamped and the overdamped mode are 7.3:1, and the corresponding parameters for ω are 8.2 and 2.2 $(\text{ps})^{-1}$ and for $\Gamma_1 = \frac{1}{2}\,\Gamma_2 = \frac{1}{2}\,\gamma$, 7.4 and 4.5 ps^{-1}, respectively. The third-order signals and the t_2-dependent fifth-order signals are well simulated, as shown in Fig. 3(b). However, the t_1 dependence of the fifth-order signal cannot be modeled at all. The square root rather than the calculated signal itself resembles the measured signal. This is shown in Fig. 3(a). Introduction of inhomogeneity of the underdamped mode considerably reduces the quality of these simulations.

For benzene, the general picture is the same. The t_2-dependent fifth-order signals point to the presence of a homogeneously broadened underdamped mode. The t_1 dependence again resembles the OKE effect, which is the square root of the response expected from the model. We therefore have to conclude that the model fails to describe the fifth-order response properly, along the t_1 time coordinate. Hence, any interpretation of the experimental results, based upon this model, should be considered with great care.

In conclusion, we observed two-dimensional fifth-order signals that differ along both time axes from third-order TGS results. The coherent part of the induced motion dominates the t_2 coordinate of the fifth-order response, while both the coherent and diffusive behavior determine the t_1 dependence of the signal. A model, based on the presence of an overdamped and an underdamped oscillator, gives a good description of the third-order TGS signal and the t_2 dependence of the fifth-order signal, but fails to describe the t_1 dependence of the fifth-order signal. This may be due to the crude separation of libration and diffusion, which are projected upon two independent harmonic motions on fixed potential surfaces. We are currently working out the nonlinear optics of models that couple coherent oscillations and diffusion in more realistic ways. It is still an unsolved problem of theoretical physics to include many body effects, which give rise to interaction-induced polarizability, into a perturbative treatment of the nonlinear optics. Within the current model, we find indications that the oscillatory motion is homogeneously broadened, implying very short memory times in the propagation of intermolecular motions in liquids.

The investigations were supported by the Netherlands Foundation for Physical Research (FOM) with financial aid from the Netherlands Organization for the Advancement of Science (NWO).

[1] D. McMorrow and W.T. Lotshaw, J. Phys. Chem. **95**, 10 395 (1991).
[2] M. Cho, M. Du, N.F. Scherer, G.R. Fleming, and S. Mukamel, J. Phys. Chem. **99**, 2410 (1993).
[3] A. Waldman, U. Banin, E. Rabani, and S. Ruhman, J. Phys. Chem. **96**, 10 842 (1992).
[4] S. Ruhman and K.A. Nelson, J. Phys. Chem. **94**, 859 (1991).
[5] B.J. Berne and R. Pecora, *Dynamic Light Scattering* (Wiley, New York, 1976).
[6] R.W. Hellwarth, Prog. Quantum Electron. **5**, 1 (1977).
[7] R.F. Loring and S. Mukamel, J. Phys. Chem. **83**, 2116 (1985).
[8] D. Vanden Bout, L.J. Muller, and M. Berg, Phys. Rev. Lett. **67**, 3700 (1991).
[9] R. Inaba, K. Tominaga, M. Tasumi, K.A. Nelson, and K. Yoshihara, Chem. Phys. Lett. **211**, 183 (1993).
[10] P.C. Becker, H.L. Fragnito, J.-Y. Bigot, C,H, Brito-Cruz, R.L. Fork, and C.V. Shank, Phys. Rev. Lett. **63**, 505 (1989).
[11] E.T.J. Nibbering, D.A. Wiersma, and K. Duppen, Phys. Rev. Lett. **66**, 2464 (1991).
[12] Y. Tanimura and S. Mukamel, J. Chem. Phys. **99**, 9496 (1993).
[13] K. Tominaga and K. Yoshihara, Phys. Rev. Lett. **74**, 3061 (1995).
[14] K. Tominaga, G.P. Keogh, Y. Naitoh, and K. Yoshihara, J. Raman Spectrosc. **26**, 495 (1995).
[15] T. Steffen and K. Duppen (to be published).
[16] S. Mukamel, *Principles of Nonlinear Optical Spectroscopy* (Oxford University Press, New York, 1995).
[17] J.A. Leegwater and S. Mukamel, J. Chem. Phys. **102**, 2365 (1995).